

The complex iron line in NGC 7469 observed by BeppoSAX

A. De Rosa,^{1,2} A. C. Fabian¹ and L. Piro²

¹*Institute of Astronomy, Madingley Road, Cambridge CB3 0HA*

²*Istituto di Astrofisica Spaziale, C.N.R., Via Fosso del Cavaliere, Roma, Italy*

ABSTRACT

In this letter we present analysis of BeppoSAX data from a long look at the Seyfert 1 galaxy NGC 7469. The presence of a soft excess below 0.8 keV is confirmed by our analysis and no warm absorber component is required to fit the spectrum. A complex iron emission line and the Compton reflection hump are clearly detected. The profile of the line is too broad to associate this feature with distant matter. In addition, the observed soft excess and the energy of the iron line $E_{Fe}=6.8$ keV strongly support a scenario in which the hard X-rays are reprocessed by a photoionized accretion disc. This hypothesis was tested fitting the BeppoSAX spectrum with the ionized disc reflection model of Ross & Fabian. A second narrow line component, in addition to that produced in the disc, is also required to fit the observed iron line profile. A high energy cut-off around 150 keV is clearly detected in the spectrum.

Key words: Galaxies: individual: NGC 7469 – Galaxies: Seyfert – X-rays: galaxies

1 INTRODUCTION

A narrow iron line component is clearly detected in recent Chandra (Kaspi *et al.* 2001, Yaqoob *et al.* 2001) and XMM observations (Reeves *et al.* 2001, Pounds *et al.* 2001) of some Seyfert 1 galaxies. These observations suggest that part of the Fe line is produced very far from the accretion disc. A strong broad iron line component is found in the X-ray spectra of many Seyfert galaxies (Fabian *et al.* 2000) by ASCA (Nandra *et al.* 1997, Tanaka *et al.* 1995, Yaqoob *et al.* 2002), XMM (Wilms *et al.* 2001) and BeppoSAX (Guainazzi *et al.* 1999, De Rosa *et al.* 2002).

The near ($z \sim 0.017$) Seyfert 1 NGC 7469 shows a very complex X-ray spectrum. EXOSAT observed a soft excess in this source (Barr 1986) which was confirmed by Einstein (Turner *et al.* 1991). Two ROSAT observations in 1991 (Turner *et al.* 1993) and 1992 (Brandt *et al.* 1993) did not resolve the origin of the soft spectral component (e.g. a soft excess, a warm absorber or a combination of the two). No evidence of a warm absorber was found in the 1993 ASCA spectrum (Guainazzi *et al.* 1994). An iron emission line and a flattening of the spectrum above 10 keV were detected by Ginga (Piro *et al.* 1990). When the spectrum above 10 keV was reproduced with a cold Compton reflection component (George & Fabian 1991; Matt, Perola & Piro 1991), the intrinsic photon index was $\Gamma = 1.99 \pm_{0.05}^{0.06}$ (Nandra 1991), while a partial covering model yielded $\Gamma = 1.92 \pm 0.03$ (Piro *et al.* 1990). The line profile was found to be narrow ($\sigma < 150$ eV) in the ASCA spectrum (Guainazzi *et al.* 1994), suggesting that the reprocessing material has to be far from the central source (several hundreds of Schwarzschild radii). Nevertheless Nandra *et al.* (1997) found marginal evidence of a broad component of the iron line in analysing the ASCA spectrum.

The broad band of BeppoSAX (Boella *et al.* 1997) is particularly suited to the deconvolution of such complex spectra. In this

letter we present the analysis of a BeppoSAX week-long observation of NGC 7469 in 1999. This spectrum was already analysed by Perola *et al.* (2002) within a sample of nine sources observed with BeppoSAX. Their analysis showed evidence of soft excess component and a not resolved iron line was also detected, indicating a component from the centre of the accretion flow.

2 OBSERVATION

BeppoSAX observed NGC 7469 from 1999 November 23 to 1999 November 29. The net exposure time in the MECS was 249180 s. The observed mean flux was $F_{2-10\text{keV}} = 3.7 \times 10^{-11} \text{ erg cm}^{-2} \text{ s}^{-1}$ for our best fit model (see Table 1). Spectra were extracted within a circular region centered on the source with radii of 4' and 6' for MECS and LECS respectively. The background was extracted from event files of source-free regions ("blank fields"). The PDS spectrum was filtered with fixed rise time. The BeppoSAX data were then fitted using the XSPEC 11.1 package. All quoted uncertainties correspond to 90 per cent confidence intervals for one interesting parameter ($\Delta\chi^2=2.71$). Each model we tested was multiplied by a normalization constant in order to take into account possible miscalibrations between the different instruments. We allowed the PDS/MECS normalization to vary between 0.77 and 0.95, while the LECS/MECS normalization ratio was running between 0.7 and 1 (Fiore, Guainazzi & Grandi 1999).

In Figure 1 we show the LECS (0.7-2.5 keV), MECS (5-10 keV) and PDS (13-200 keV) lightcurves, the hardness ratio MECS (5-10 keV) / MECS (3-10 keV) is also plotted in the last panel. In each plot we reported the χ^2/dof for a constant hypothesis. Even if the source showed flux variability in the soft, medium and hard energy range ($P_{\chi^2} \ll 10^{-3}$ for LECS, MECS and PDS lightcurves), the MECS hardness ratio (which is in the energy range of interest

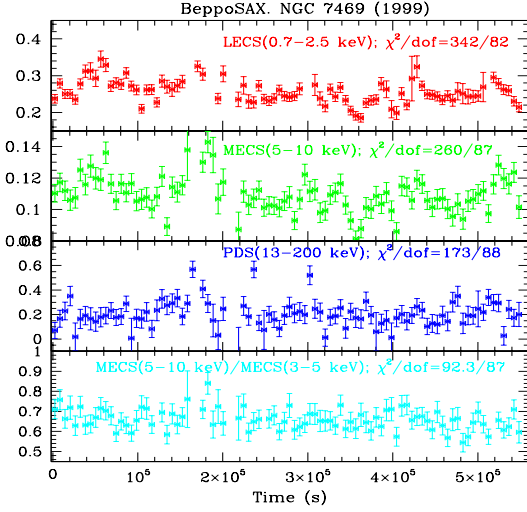


Figure 1. LECS, MECS, PDS lightcurves and MECS hardness ratio of BeppoSAX observation of NGC 7469. In each panel is indicated the χ^2/dof for a constant hypothesis.

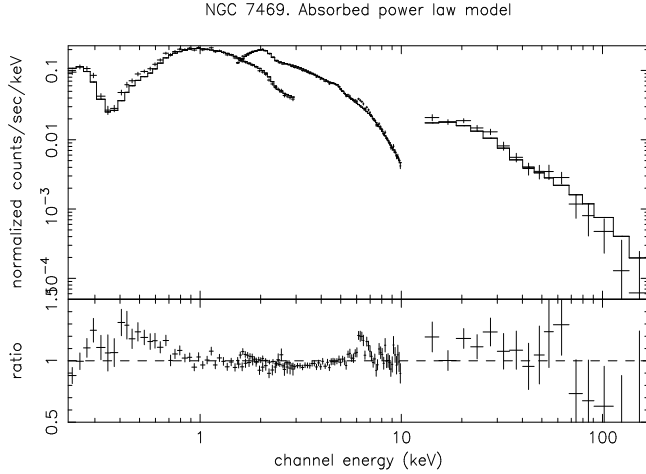


Figure 2. LECS, MECS and PDS data (upper panel), and data/model ratio (lower panel) in the case of an emission continuum fitted with a power law absorbed by a cold galactic gas.

to investigate the Fe line behaviour) is in good agreement with a constant value ($P_{\chi^2} = 0.33$). A detailed discussion about the complex spectral variability in NGC 7469 (Nandra & Papadakis 2001 and references therein), is beyond the focus of this letter.

3 RESULTS

We fitted the LECS (0.2-3 keV), MECS (1.5-10 keV) and PDS (13-200 keV) data simultaneously. In Figure 2 we show the data and data/model ratio when the whole BeppoSAX spectrum is fitted by an absorbed ($N_H = 4.8 \times 10^{20} \text{ cm}^{-2}$ the Galactic value from Elvis *et al.* 1989) power law. This model is clearly inadequate, with several features emerging from the spectra: an excess at energy less than 1 keV, an iron line component with the Compton reflection hump, and a deficit of counts above 70 keV.

The baseline model we employed to fit the data consisted of an absorbed cut-off power law, a cold reflection component (PEXRAV

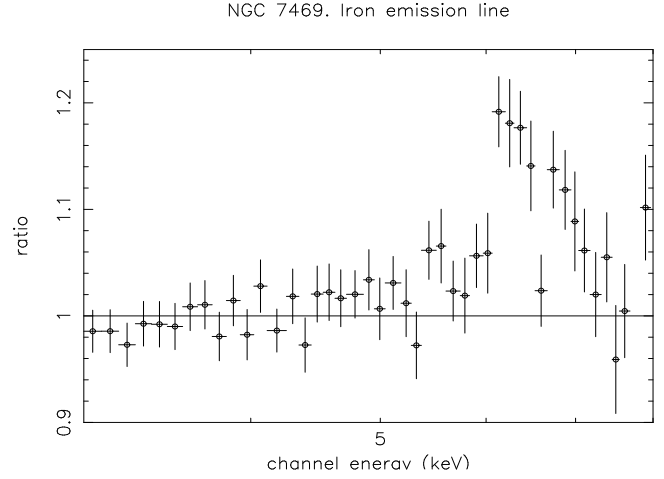


Figure 3. Ratio data/model of the iron line when the data are fitted with the baseline model in the whole BeppoSAX band except the 4-7.5 keV energy range.

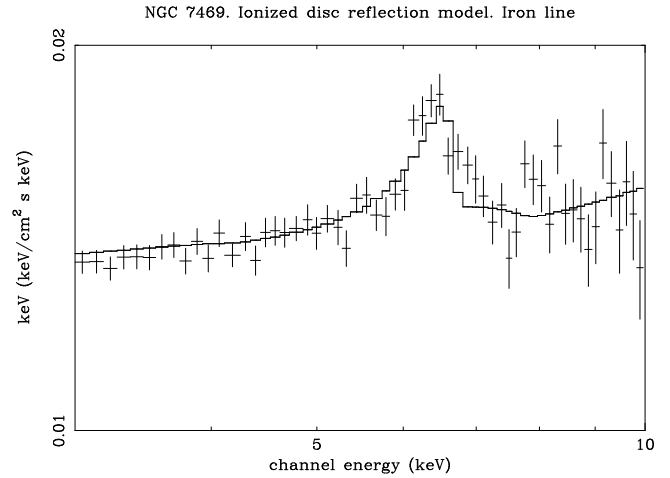


Figure 4. The unfolded BeppoSAX/MECS spectra of NGC 7469 is plotted with the ionized disc reflection model with solar Fe abundance (see Table 2). Clear residuals around the Fe line can be observed.

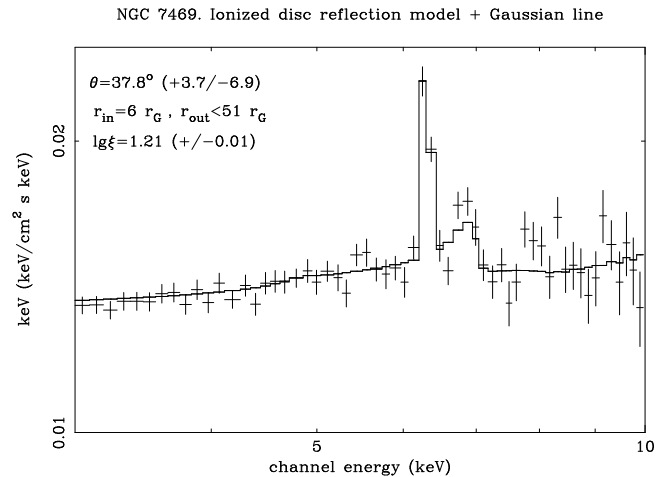


Figure 5. A similar plot to Figure 4 but with the spectrum fitted with an ionized reflection model plus a gaussian component.

Table 1. Cold disc reflection model. ^(b) The inclination angle is linked to that of the reflection component and frozen to 30°. ^(•) Gravitational radius $R_G = GM/c^2$. ^(*) In this model for the narrow component $E_L = 6.3$ keV and $\sigma = 0$ keV. All the line energies are quoted in the source rest frame.

Model	kT_{BB} (eV)	Γ	R	$E_{cut-off}$ (keV)	E_L (keV)	σ or R_{out} (keV) or ($\bullet R_G$)	EW (eV)	χ^2/dof
Single gaussian	$80 \pm 8_4$	$2.07 \pm 0.03^{0.02}$	1.49 ± 0.40	245 ± 117^{693}	$6.42 \pm 0.11^{0.12}$	> 0.39	175 ± 80	151.3/136
Diskline ^b	84 ± 9	2.06 ± 0.02	$1.4 \pm 0.3^{0.2}$	260 ± 100^{630}	$6.60 \pm 0.25^{0.16}$	> 52	180 ± 70	155.5/136
Diskline ^b + Narrow gaussian [*]	$84 \pm 7_9$	2.06 ± 0.02	$1.8 \pm 0.4^{0.6}$	140 ± 33^{385}	6.82 ± 0.15	> 15	121 ± 100 75 ± 40	142.9/134

Table 2. Ionized disc reflection model. The exponent for the disc emissivity law r^β is frozen to the value $\beta = -3$. ^(†) Parameter fixed during the fit. ^(‡) Parameter pegged at upper limit.

Model	Γ	$\log \xi$	R	θ (°)	$\dagger r_{in}$ (R_G)	r_{out} (R_G)	E_L (keV)	χ^2/dof
Ionized disc	2.01 ± 0.02	$1.08 \pm 0.19^{0.08}$	$0.95 \pm 0.09^{0.04}$	$20.6 \pm 8.6^{6.6}$	6	$\dagger 10^7$	-	169/139
Ionized disc + gaussian	2.02 ± 0.02	1.21 ± 0.02	$0.87 \pm 0.08^{0.10}$	$37.8 \pm 6.9^{3.7}$	6	< 51	6.30 ± 0.05	151.9/137
ASCA								
Ionized disc + gaussian	2.02 ± 0.03	$1.08 \pm 0.42^{0.08}$	1 (frozen)	< 40	6	$\dagger 10^7$	6.36 ± 0.06	399.3/378

in XSPEC Magdziarz & Zdziarski 1995) and a black body to reproduce the excess at low energy. The probability to exceeding F with the addition of the high energy cut off in the baseline model is $P_F \sim 96.5$ per cent. In Figure 3 the MECS data/model ratio is shown when the baseline model is applied to the whole BeppoSAX band, but excluding 4-7.5 keV energy range where a relativistic iron line is expected to be present. The ratio in Figure 3 shows clearly the presence of a complex iron line. We tried several models to fit the line profile and all the best fit parameters are shown in Table 1. A single gaussian is clearly inadequate ($\chi^2/dof=151.3/136$). The second step was to substitute an unphysical broad gaussian component with a physical model for a relativistic profile of the line (DISKLINE in XSPEC, Fabian *et al.* 1989). The model is still inadequate to reproduce the line residuals ($\chi^2/dof=155.5/136$). The addition of a second narrow gaussian component at the energy of the neutral iron yields a significant decrease of χ^2 ($\Delta\chi^2=13$ with the addition of 2 free parameters. $P_F=99.70$ per cent). The EW was 121 ± 100 eV and 75 ± 40 eV for the broad and narrow components respectively. The centroid of the relativistic line $E_L=6.82 \pm 0.15$ keV, indicates He-like iron.

Two gaussian narrow lines give a fair χ^2 ($\chi^2/dof=142/135$). The second line (EW=57±36 eV) lies to the energy of highly ionized iron $E=6.94 \pm 0.21^{0.12}$ keV, i.e. H-like iron. This component has to be produced in a gas characterized by an ionization parameter $\xi = 4\pi L_{ion}/n_e R^2 > 2000$ erg cm s⁻¹ (Matt *et al.* 1996). Assuming a temperature $T=10^6$ K, the total recombination rate to all states for FeXXVI is $\alpha_{tot} = 2.4 \times 10^{-11}$ cm³ s⁻¹ (Seaton 1959), and the line emissivity is $J_{line} = \frac{n_e^2}{4\pi} A_{Fe} y h\nu \alpha_{tot}$, with A_{Fe} and y the iron abundance and the iron effective fluorescent yield respectively. In the case of a simple spherical geometry if we assume a ionizing luminosity $L_{ion} \sim 10^{43}$ erg s⁻¹, and with the observed H-like iron line luminosity $L_{line} \sim 10^{41}$ erg

s⁻¹, we can estimate a lower limit to the electron number density $n_e > (\frac{3L_{line}}{A_{Fe} y E_{line} \alpha_{tot}})^2 \times (\frac{L_{ion}}{\xi})^{-3} = 2.4 \times 10^{10}$ cm⁻³ (assuming $A_{Fe} = 3.3 \times 10^{-5}$ of Morrison & McCammon 1983 and $y \sim 0.63$ by Matt *et al.* 1993b for a temperature of 10^6 K) and then an upper limit for the distance of the gas from the ionizing central source, $R < 7 \times 10^{14}$ cm. This means that such gas must lie within few hundred Schwarzschild radii ($R_s=2GM/c^2$) of the central black hole (assuming a mass for it of $\sim 10^7 M_\odot$, Wandel *et al.* 1999).

The fit with two gaussian emission lines (one narrow) is still perfectly acceptable ($\chi^2/dof=133/134$), nevertheless the extremely large value of the intrinsic width of the broad component ($\sigma=1.8 \pm 0.7^{1.0}$ keV) indicates a poor description of the continuum at the energy of the line. Thus we are lead to believe that a diskline + gaussian component is a more suitable and physically consistent model to reproduce the Fe emission line observed in NGC 7469.

The presence of an ionized iron line and of a soft emission component, together with an unusual value of the relative reflection, significant greater than 1 ($R=1.8 \pm 0.6^{0.4}$, see Table 1), strongly suggests the hypothesis that all these features could be the result of hard X-ray reprocessing in a hot ionized accretion disc (Matt *et al.* 1993a, 1996, Ross, Fabian & Young 1999, Nayakshin *et al.* 2000, Ballantyne *et al.* 2001). We tested an ionized reflection model which takes into account the reflected spectrum of the disc in the whole BeppoSAX energy range. The model we employed was that of Ross & Fabian (1993). The most important quantity in determining the shape of the reflected continuum is the ionization parameter $\xi = 4\pi F_X/n_H$, where F_X is the X-ray flux (between 0.1-100 keV) illuminating a slab of gas with solar abundances and constant hydrogen number density $n_H=10^{15}$ cm⁻³. The incident flux is assumed be a power law with spectral photon index Γ and a high energy cut-off at 100 keV. The computed reflected spectrum is multiplied for a factor R (“reflected fraction”) and added to the

primary continuum. This model includes the Fe K α emission line and the spectral features at low energy (emission lines and recombination continuum). Larger values of ξ indicates a more ionized disc which will affect the strength and width of the iron line (Matt *et al.* 1993a, 1996), and the absorption edges. The soft emission from the accretion disc is not taken into account to determine the reprocessing features. During the fit we applied to the spectrum a relativistic blurring appropriate for a Schwarzschild geometry assuming a disc emissivity law (Fabian *et al.* 1989).

Fitting the spectrum with an ionized disc model (see Table 2) with solar Fe abundance does not give a satisfactory result ($\chi^2/dof=169/139$). Clear residuals can be observed at the energy of the iron line (see Figure 4). To increase the Fe emissivity to reproduce the observed strength of the line we tried to fit the data with an ionized reflection model with 2 and 5 times solar Fe abundances. Nevertheless these models are inadequate to fit the soft part of the spectrum, and the result of the fit is poor ($\chi^2/dof_{(2XFe)}=187/139$, $\chi^2/dof_{(5XFe)}=205/139$). A better model to reproduce the iron line residuals is to add a narrow line component. The ionized disc model with an additional gaussian component finally give us a good fit ($\Delta\chi^2=17$ for the sum of two interesting parameters. $P_F=99.97$ per cent) and no large residuals can be found at the energy of the iron line (see Figure 5). The best fit parameters for the several ionized reflection models we employed are shown in Table 2. In Figure 6 we plot the confidence contours (68, 95 and 99 per cent) Reflection fraction and photon index for the ionized disc plus gaussian line model.

No additional (cold or ionized) iron edge is required to fit the spectrum. If we add an absorption edge with the energy fixed to the value for cold iron $E_{edge}=7.1$ keV, the fit worsens and we find a very low upper limit for the optical depth $\tau < 0.01$.

The soft excess at low energy can not be accounted for by a warm absorber component. If we substitute the black body in the last model in Table 1, with two absorption edges at the energy of the OVII (0.74 keV) and OVIII (0.87 keV), the fit is worse ($\chi^2/dof=150/134$). The same result is obtained using a more detailed description of the warm absorber with ABSORI model in XSPEC. A warm absorber component is not required to fit the low energy data of NGC 7469 ($P_F=34$ per cent).

Piro *et al.* (1990) showed that the GINGA spectrum of NGC 7469 observed in 1988 could be reproduced by a “partial covering” model (Holt *et al.* 1980). In this scenario an absorbing medium is supposed to cover only a fraction f_{cov} of the central source with a column density N_{Hcov} . The direct X-ray would be blocked at low energy, but would penetrate through the absorbing gas above 5 keV imprinting the curvature in the observed spectrum. Nevertheless Leighly *et al.* (1996) showed that this model was not able to explain the observed flux and spectral variability in NGC 7469.

When we model the BeppoSAX spectrum of NGC 7469 with partial covering the fit is fair ($\chi^2/dof=142.7/136$), with $N_{Hcov} = (5 \pm 1) \times 10^{23} \text{ cm}^{-2}$ and $f_{cov} = (0.32 \pm 0.04)$, and the EW of the iron line $EW=69 \pm 20$ eV. Nevertheless the expected value of the equivalent width for an optically thin medium illuminated by an isotropic continuum, with a Fe solar abundance and the N_{Hcov} and f_{cov} obtained by BeppoSAX observation, is in the range 100-200 eV, i.e. larger than that observed in the spectrum. This evidence together with the complex profile of the Fe line and the soft X-ray excess, make the reflection from a (possibly ionized) accretion disc the most appealing scenario.

4 DISCUSSIONS AND CONCLUSIONS

The BeppoSAX long look at NGC 7469 shows a very complex X-ray spectrum. Both a soft excess component and reprocessing features are detected. The continuum emission can be reproduced either with a cold reflection model and a black body component (with temperature $kT \sim 84$ eV fully consistent with that measured by ASCA, Guainazzi *et al.* 1994) or with an ionized disc reflection model that takes into account the disc emissivity below 0.8 keV. Whichever model we employ to fit the spectrum, the observed iron line requires a complex profile which is hard to associate with a distant reflector. In addition the energy of the relativistic line $E=6.8$ keV corresponds to high ionized iron that can not be reconciled with the cold disc scenario.

An ionized iron line component was already observed by XMM in Mkn 509 (Pounds *et al.* 2001), Mkn 205 (Reeves *et al.* 2001) and NGC 5506 (Matt *et al.* 2001). In this last source a solution in term of a blend of He- and H- like narrow iron line is preferable to that of a relativistic ionized disc, but in Mkn 509 and Mkn 205 this feature was explained in terms of an ionized accretion disc. In the case of NGC 7469 the predicted iron line component from the ionized disc model does not fit the whole observed profile. A narrow line component has to be included in the model. The origin of this second component is still a matter of debate. It has been detected in many Seyfert 1s observed so far by Chandra (Kaspi *et al.* 2001, Yaqoob *et al.* 2001) and XMM (Pounds *et al.* 2001, Reeves *et al.* 2001). It is associated with a region distant from the central source and probably coincident either with a Compton thick gas, e.g. the “torus” obscuring the Seyfert 2s (Antonucci 1993, Ghisellini *et al.* 1994) or with the Compton thin BLR. At least in the cases of NGC 4051 (Guainazzi *et al.* 1998) and NGC 5506 (Matt *et al.* 2001) the narrow core of the iron line was associated to a Compton thick gas. Nevertheless the bulk of the Compton reflection in NGC 7469 can be completely associated with the ionized disc (see Figure 6) iron component. In fact with the combination of a cold and an ionized Compton reflection we obtained a very poor fit ($\chi^2/dof=156.4/135$).

Even if a partial covering model can reproduce the observed BeppoSAX spectrum, the value of the equivalent width of the iron line predicted in this model is significantly larger than that measured. This could require that the covering medium has a small solid angle at the source.

A warm absorber component is not required to fit the BeppoSAX low energy spectrum, this allowed us to detect the redward extent of the iron line, and thus constrain the inner radius of the disc.

A double iron line component also can reproduce the observed profile. We cannot rule out the possibility that the second H-like iron component is created in a warm ($T \sim 10^6$ K) gas within a few 100s R_s of the central source.

Finally to check our results we fitted the the ASCA spectrum above 1 keV (SIS0 and GIS2, sequence number 71028030, from the Tartarus database) with an ionized disc reflection model. The fit was good ($\chi^2/dof=399.3/378$) and the ionization parameter was consistent with that observed in the BeppoSAX spectrum, $\log \xi_{ASCA} = 1.08 \pm 0.42_{0.08}$. A narrow line component also is really marginally required ($P_F=92$ per cent) to fit the Fe line. The flux of this component was the same in the two observations, while the flux in 2-10 keV was higher by 30 per cent during the SAX long look. Nevertheless the uncertainty on the line intensity renders any result about variability inconclusive.

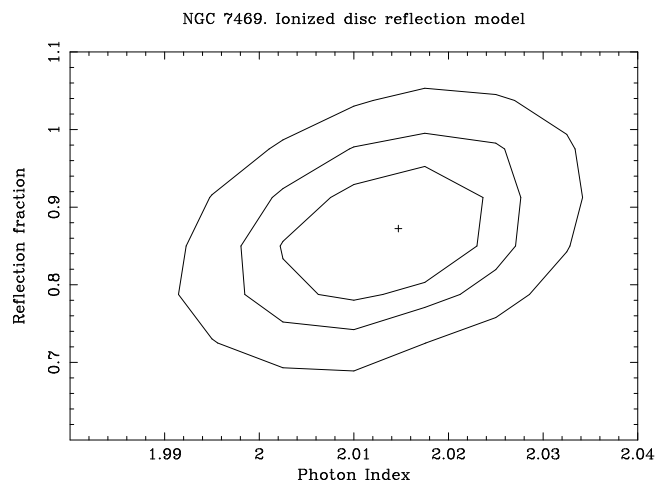


Figure 6. 68, 95 and 99 per cent confidence contours Reflection fraction *vs* photon index for the ionized disc plus gaussian line model. The “+” denotes the best fit values of R and Γ .

ACKNOWLEDGMENTS

We thank David Ballantyne for computing the grid of ionized disc models. A.D.R acknowledges the European Association for Research in Astronomy (EARA) Marie Curie for financial support. The BeppoSAX satellite is a joint Italian-Dutch program.

REFERENCES

- Antonucci R., 1993, *ARA&A*, 31, 473
 Ballantyne D., Ross R.R., Fabian A.C., 2001, *MNRAS*, 327, 10
 Barr P., 1986, *MNRAS*, 223, 29p
 Boella G., Butler R.C., Perola G.C., Piro L., Scarsi L., Bleeker J., 1997, *A&A* 122, 299
 Brandt W.N., Fabian A.C. Nandra K., Tsuruta S., 1993, *MNRAS*, 265, 996
 De Rosa A., Piro L., Fiore F., Grandi P., Maraschi L., Matt G., Nicastro F., Petrucci P.O., 2002, *A&A*, 38, 838
 Elvis M., Lockman F.J., Wilkes B. 1989, *AJ*, 97, 777
 Fabian A.C., Rees M.J., Stella L., White N.E., 1989, *MNRAS*, 238, 729
 Fabian, A.C., Iwasawa K., Reynolds C.S., Young, A.J., 2000, *PASP*, 112, 1145
 Fiore F., Guainazzi G., Grandi P. 1999, *Cookbook for BeppoSAX NFI Spectral analysis*. SDC report. (Available from <http://asdc.asi.it/bepposax/software/index.html>)
 George I.M. & fabian A.C., 1991, *MNRAS*, 249, 352
 Ghisellini F., Haardt F., Matt G., 1994, *MNRAS*, 267, 743
 Guainazzi M., Matsuoka M., Piro L., Mihara T., Yamauchi M., 1994, *ApJ*, 436, L35
 Guainazzi M., Nicastro F., Fiore F., Matt G., McHardy I., Orr A., Barr P., Fruscione A., Papadakis I., Parmar A.N., Uttley P., Perola G.C., Piro L., 1998, *MNRAS*, 301, L1
 Guainazzi M., Matt G., Molendi S., Orr A., Fiore, F., Grandi P., Matteuzzi, A., Mineo, T., Perola G.C., Parmar A.N., Piro L., 1999 *A&A*, 341, L27
 Holt S.S., Mushotzky R.F., Boldt E.A., Serlemitsos P.J., Becker R.H., Szymkowiak A.E., White N.E., 1980, *ApJ*, 241, L13
 Kaspi S., Brandt W.N., Netzer H., George I., Chartas G., Behar E., Sambruna R., Garmire G. and Nousek J. 2001, *ApJ*, 554, 216
 Leighly K., Kunieda H., Awaki H., Tsuruta S., 1996 *ApJ*, 463, 158
 Magdziarz P. & Zdziarski A.A. 1995, *MNRAS*, 273, 837
 Matt G., Perola G.C., Piro L. 1991, *A&A*, 247, 25
 Matt G., Fabian A.C., Ross R.R., 1993a, *MNRAS*, 262, 179
 Matt G., Brandt W.N. and Fabian A.C., 1993b, *MNRAS*, 280, 823
 Matt G., Fabian A.C., Ross R.R., 1996, *MNRAS*, 278, 1111

- Matt G., Guainazzi M., Perola G. C., Fiore F., Nicastro F., Cappi M., Piro L., 2001b, *A&A*, 377, L31
 Morrison R. & McCammon D., 1983, *ApJ*, 270, 119
 Nandra K., 1991, PhD thesis, Leicester University
 Nandra, K., George I.M., Mushotzky R.F., Turner T.J., Yaqoob, T., 1997, *ApJ*, 477, 602
 Nandra K. & Papadakis I.E., 2001, *ApJ*, 554, 710
 Nayakshin S., Kazanas D., Kallmann T., 2000, *ApJ*, 537, 833
 Perola G.C., Matt G., Cappi M., Fiore F., Guainazzi M., Maraschi L., Petrucci P.O., L. Piro, 2002, *A&A*, accepted, astro-ph/0205045
 Piro L., Yamauchi M. & Matsuoka M., 1990, *ApJ*, 360, L35
 Pounds K., Reeves J., O'Brien P., Page K., Turner M., Nayakshin S., 2001, *ApJ*, 559, 181
 Reeves J.N., Turner M., Pounds K., O'Brien P., Boller Th., Ferrando P., Kendziorra E., Vercellone S., 2001, *ApJ*, 365L, 134
 Ross R.R., Fabian A.C., Young A.J., 1999, *MNRAS*, 306, 461
 Ross R.R. & Fabian A.C., 1993 *MNRAS*, 261, 74
 Seaton M.J., 1959, *MNRAS*, 119, 81.
 Tanaka Y., Nandra K., Fabian A.C., Inoue H., Otani C., Dotani T., Hayashida K., Iwasawa K., Kii T., Kunieda H., Makino F., Matsuoka M., 1995, *Nature*, 375, 659
 Turner T.J., Weaver K.A., Mushotzky R.F., Holt S.S., Madejeski G.M., 1991, *ApJ*, 381, 85
 Turner T.J., George I.M., Mushotzky R.F., 1993, *ApJ*, 412, 72
 Yaqoob, T., George I.M., Nandra K., Turner T.J., Serlemitsos P.J., Mushotzky R.F., 2001, *ApJ*, 546, 759
 Yaqoob T., Padmanabhan U, Dotani T, Nandra K., *ApJ*, accepted. astro-ph/0112318
 Wandel A., Peterson B.M. and Malkan M.A., 1999, *ApJ*, 526, 579.
 Wilms J., Reynolds C.S., Begelman M.C., Reeves J., Molendi S., Staubert R., Kendziorra E., 2001, *MNRAS*, 328, L27

This paper has been typeset from a \TeX / \LaTeX file prepared by the author.